Computer simulation of structure and microphase separation in model *A*-*B*-*A* triblock copolymers

M. Banaszak,[1,*] S. Wołoszczuk,[1] T. Pakula,[2] and S. Jurga[1]

[1]*Macromolecular Physics Laboratory, Institute of Physics, A. Mickiewicz University, ulica Umultowska 85, 61-614 Poznan, Poland*

[2]*Max-Planck-Institute for Polymer Research, P.O. Box 3148, D-55021 Mainz, Germany*

(Received 15 April 2002; revised manuscript received 2 July 2002; published 30 September 2002)

A set of computer simulations for three symmetric *A*-*B*-*A* triblock copolymer microarchitectures at varying temperatures is reported. By using the cooperative motion algorithm we obtain energy, specific heat, end-to-end distance, and bridging fraction as a function of the reduced temperature. The order-disorder transition temperatures are determined, an outline of a symmetric *A*-*B*-*A* triblock copolymer phase diagram is presented, and the visualization of different microstructures is given. A bicontinuous microstructure is reported at 67% fraction of *A* component.

DOI: 10.1103/PhysRevE.66.031804 PACS number(s): 83.80.Uv

I. INTRODUCTION

Block copolymers have been extensively studied in recent years due to their fascinating ability to self-assemble into a variety of ordered mesoscopic structures [1–28]. Self-assembly indicates the ability of a given system to grow islands of one of the components to the mesoscopic size (about a few tens of nanometers), and then stabilize the growth, so that phase separation occurs only on a mesoscale, rather than a macroscale. Traditionally copolymers have been used as compatibilizers and surfactants, but recently they have found their way into nanotechnology. By engineering molecular weight, molecular architecture, and composition one can control the size and morphology of these nanostructures.

Ordered microstructures of *A*-*B* diblock copolymers have been studied both theoretically [11–13,20,21,29], and experimentally for many years [6,7,9,19]. They also have been investigated by numerous computer simulations, e.g., Refs. [8,10,14–16,22,23]. Their basic thermodynamic and mesoscopic behavior is reasonably well understood.

Diblock copolymer self-assembly or ordering takes place as those copolymers are cooled down from a disordered high-temperature phase to a low-temperature ordered phase. This process is called order-disorder transition (ODT) or also microphase separation transition, and is characterized by a temperature T_{ODT}, which marks the onset of long range order. It is well established experimentally that the microphase (ordered phase) can look like an array of bcc spheres, hexagonally packed cylinders, or spatially ordered layers. These microphases are often referred to as the ''classical'' microstructures. Close to the ODT, the interface between the microdomains is diffused, and interfaces can fill up most of the space. This segregation regime is called weak segregation limit. By contrast, when the interfaces between microdomains are sharp and highly localized the system is in strong segregation limit. While the pure diblock copolymer microstructure depends on the interplay of entropic and enthalpic effects, at low temperatures it is mostly determined by enthalpic, and therefore volumetric considerations. For copolymer blends and solutions, where the system tends to separate into distinct macrophases at lower temperatures, phase behavior is more complex. Pure diblocks with roughly the same volume of both species form layers (lamellae) at lower temperatures, while diblocks with significant (more than about 80% or less than 20% by volume) excess of one species form ordered spheres (micelles). The diblocks with intermediate volume fractions usually form hexagonally packed cylinders. Apart from those classical microstructures there have been discovered complex microstructures such as ordered bicontinuous double diamond structure ($Pn\bar{3}m$ space group), gyroid bicontinuous structure ($Ia\bar{3}d$ space group), and hexagonally perforated layers. There was some controversy about the existence and thermodynamic stability of those complex microstructures, and now only the gyroid microstructure is known to be a stable complex phase for pure diblock copolymers. The experimental phase diagram of a real diblock copolymer can be found in, e.g., Ref. [6], and the corresponding theoretical phase diagram was calculated using self-consistent field theory (SCFT) [12]. The gyroid microstructure is stable in a narrow volume fraction window between layers and cylinders at roughly 30% or 70% by volume, and it is a bicontinuous cubic structure in which the minority component microdomains form interweaving left- and right-handed threefold coordinated lattices. The bicontinuous double diamond microstructure, on the other hand, is a cubic structure in which the minority component microdomains form interweaving fourfold coordinated lattices. The double diamond microstructure is known to be metastable, and has been reported in the same narrow volume fraction window as the gyroid microstructure.

While the properties and phase diagram for *A*-*B* diblock copolymers are fairly well understood, this is not the case for *A*-*B*-*C* triblock copolymers. *A*-*B*-*C* triblock copolymers consist of three different polymer blocks (Fig. 1), and since there are three interaction parameters as opposed to one interaction parameter in *A*-*B* diblock copolymers, the microstructures and phase behavior of triblocks is much more complex. For example, the morphological structure (microstructure) of triblock copolymers depends not only on the temperature, the overall molecular weight, and the fraction of each block, but also on the sequence of the blocks in the

*Electronic address: mbanasz@amu.edu.pl

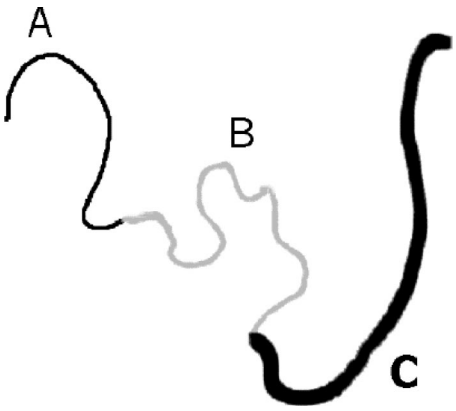

FIG. 1. A schematic picture of an *A-B-C* triblock copolymer chain.

chain. In addition to well-established microstructures, known from the diblock studies, there are new intriguing morphologies, such as a lamella-cylinder combination microstructure, a lamella-sphere combination microstructure, and a cylinder-ring combination microphase. These combination morphologies, which often have characteristics of one-, two-, three-dimensional order simultaneously, can have unusual electronic and transport properties. In this paper, we limit out attention to symmetric *A-B-A* triblock copolymers, where the third block is made of the same species as the first block, i.e., the *A* block, and both the *A* end blocks are of the same volume. Such triblocks have been studied by many workers [3] (and references therein), and of particular interest is a recent work by Matsen and Thompson [5] where a phase diagram for symmetric *A-B-A* triblock copolymer melt is calculated using the SCFT. These authors show that the topology of triblock phase diagram is the same as that for the corresponding diblock, with very similar phase boundaries between lamellar and gyroid microphases, between gyroid and cylindrical microphases, and between cylindrical and spherical microphases. This phase diagram is roughly symmetric with respect to swapping *A* and *B* monomers.

While the thermodynamic properties of the corresponding *A-B* and symmetric *A-B-A* copolymers are quite similar, their mechanical properties are quite different. This is because the distinct feature of *A-B-A* triblock copolymers is that *B* block ends are constrained to an interface. In the ordered microphase one can, therefore, distinguish between bridged and looped configurations. In a looped configuration both ends of the *B* block are located on the same interface, whereas in the bridged configuration the two ends reside on different interfaces [5].

The aim of this study is to determine the thermodynamic and structural properties of a set of selected symmetric *A-B-A* triblock copolymers using the cooperative motion algorithm (CMA) developed by Pakula and co-workers [8–10].

We investigate *A-B-A* triblock copolymers by measuring both thermodynamic and structural properties. There are many ways of determining the ODT for block copolymers, and we did try some of them. First of all, we looked at the energy per lattice site. Second, we looked at the energy fluctuations leading to determination of the specific heat which gives a strong signature of the ODT, and third we measured the equilibrium end-to-end distance of the triblock copolymer chain which should significantly increase as the system undergoes the ODT. Finally we visualize the selected equilibrium microstructures of the triblock copolymer system.

Computer simulations are useful because they can help in diminishing the limitations of both the experiment and the theory. In experiment, it is difficult to determine copolymer phase behavior due to long relaxation times of high molecular weight copolymers and difficulties in preparation of well-characterized samples. The SCFT calculations, on the other hand, require a microstructure symmetry assumption prior to the free energy evaluation, and usually do not go beyond the mean field approximation. Drolet and Fredrickson [27,29], however, have recently proposed a new real-space implementation of SCFT which starts from a random, disordered initial condition to produce a variety of microphases with different symmetries. Computer simulation offers methods which can, in principle, be free of those drawbacks, but, unfortunately, they are still limited by available computing resources. However, with increasing computing power, and rapid development of novel simulation techniques, the results of computer simulations are bound to contribute significantly towards a better understanding of the equilibrium self-assembly of copolymers. At this moment copolymer simulations are still constrained by finite-size effects and relatively short chains (low copolymer molecular weights) due to rather small simulation box sizes which can be used meaningfully. Similarly as in experimental studies long relaxation times prevent us from reaching the thermal equilibrium, and the copolymer system is often trapped in a metastable state. Another challenge in simulations of mesoscopic self-assembly of copolymers is the competition of different length scales, i.e., simulation box size, microstructure periodicity, and the fluctuation correlation length. Micka and Binder have shown that this competition makes the straightforward application of finite-size scaling techniques impossible, unlike the case of homopolymer blends [22]. The box size should be chosen to be significantly larger than the microstructure length, but this is often quite difficult to achieve due to prohibitively long relaxation times. In order to increase efficiency many researchers use lattice models for copolymer melts, e.g., Refs. [9,10,22,23], which speed up the simulations by taking advantage of the integer arithmetic, but also introduce some error due to the symmetry of the lattice. Another method of speeding up the simulations is the application of soft potentials [28] and phantom chains [15].

Computer simulations in this study have been performed using the CMA, which has been described in detail elsewhere [9,10]. The CMA allows the simulation of a dense polymer melt on a fcc lattice with the standard periodic boundary conditions. The lattice is completely occupied by N_a monomeric units ($N_a = N_x N_y N_z/2$), and the units in each chain are connected by $(N-1)$ bonds of constant length which are not allowed to be broken or stretched. The fcc lattice sites have the coordinates (n_x, n_y, n_z), where the sum $(n_x+n_y+n_z)$ is an even number, and $n_x = 0,1,\ldots,(N_x-1)$; $n_y = 0,1,\ldots,(N_y-1)$; $n_z = 0,1,\ldots,(N_z-1)$, where

N_x, N_y, N_z are simulation box lengths and they are also even numbers. The chains satisfy the excluded volume condition. In this work two types of monomeric units (A and B) are considered. The interaction parameters between neighboring monomeric units are ϵ_{ij}, where $\epsilon_{AA}=\epsilon_{BB}=0$, and $\epsilon_{AB}=\epsilon$. The single parameter ϵ serves here as an energy unit, therefore we can define the reduced dimensionless interaction parameters, $\epsilon_{ij}^*=\epsilon_{ij}/\epsilon$. The reduced dimensionless temperature can be expressed as $T^*=k_BT/\epsilon$, and the Flory interaction parameter χ is $\chi=(z-2)\epsilon/(k_BT)$ [8]. The energy of one unit is given by the sum over all z nearest neighbors, which can be of either type A or type B. In this simulation, a dense system of triblock chains is moved by cooperative rearrangements. These moves are strictly cooperative, as in the dense system all lattice sites are occupied, and a segment of one chain can only move if other segments move simultaneously. The simulations, in this work, are performed on a fcc lattice in the $60\times30\times30$ box (that is $N_x=60$, $N_y=30$, $N_z=30$), which has the coordination number $z=12$, and the bond length $a=\sqrt{2}$, using the standard periodic boundary conditions.

Triblock A-B-C copolymers have already been investigated in computer simulations, e.g., by Dotera and Hatano [15] who were able to form a tricontinuous double diamond, using a Monte Carlo method. Their method, unlike the CMA used in this study, allows polymer chains to transparently pass through like phantom chains and requires a significant fraction of lattice vacancies, and this results in unphysical dynamics. Extensive work on diblock copolymers by Binder and coworkers, e.g. Refs. [22,23], have revealed both the advantages and limitations of lattice Monte Carlo simulations which use fluctuating bond theory and require a significant fraction of vacancies. Recently also Huh *et al.* [26], using the Metropolis sampling [30] and slithering snake algorithm, have found the A-B-A symmetric copolymer bridging function as a function of N/T^* on a $40\times40\times40$ lattice for 8-16-8 microarchitecture. This method, again unlike the CMA, requires a significant fraction of vacancies. Since the lattice methods introduce effects due to the symmetry of the lattice, one may want to get rid of those effects by performing off-lattice simulations. These are particularly useful when used in N-P-T ensemble, where pressure tensor can be kept constant, while the simulation box size varies to achieve the true equilibrium periodicity. Thus the box length becomes easily commensurate with the microstructure periodicity. This technique has been used to produce the lamellar microstructure for diblock copolymers by Grest *et al.* [31], and also by Banaszak and Clarke [32] for ionic diblock copolymers. Another promising method is the dissipative particle dynamics [28] which has produced many interesting results for block copolymers. This method uses a very soft repulsive potential, and can be regarded as a mesoscopic, massively coarse-grained model.

II. SIMULATION

In order to generate equilibrium states in this simulation, the triblock system of chains is moved by strictly cooperative rearrangements on a fcc lattice with the bond length equal to $\sqrt{2}$, and the coordination number $z=12$, using the standard periodic boundary conditions.

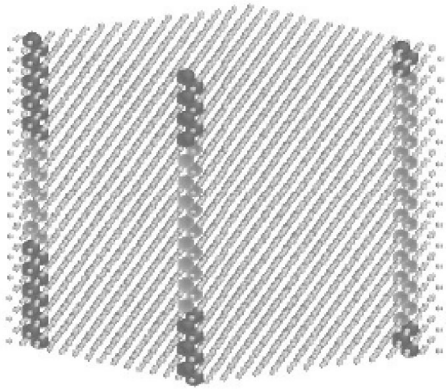

FIG. 2. Three different A-B-A triblock chains, 3-24-3, 7-16-7, and 10-10-10, placed in a $30\times30\times30$ simulation box.

In this study we present three model 30-segment ($N=30$) A-B-A copolymer microarchitectures, shown, in Fig. 2, on a $30\times30\times30$ lattice which is smaller than the actual $60\times30\times30$ lattice that is the stage of the performed simulations. In the first series of simulations we have an A block of three segments of monomeric unit of type A, followed by 24 units of type B, and terminated with a block of three units of type A. This model is to be referred in this paper as 3-24-3 triblock. Moreover we have a 7-16-7 triblock consisting of 7, 16, and 7 segments of types A, B, and A, respectively, and finally a 10-10-10 triblock consisting of 10, 10, and 10 segments of types A, B, and A, respectively. For each of the three triblock copolymer microarchitectures, we have placed 900 triblock chains, on the fcc lattice within the $60\times30\times30$ simulation box, that is $N_x=60$, $N_y=30$, $N_z=30$.

Moving a chain element alters the local energy because the monomers are in close contact with new neighbors. An attempt to move a single monomer is assumed to define a single Monte Carlo step and the probability of motion is related to the interaction energy of the monomer in the attempted position, $E_{n,final}^*$. At a given temperature T^*, the Boltzmann factor $p=\exp[-E_{n,final}^*/T^*]$ is compared with the random number r $(0\leqslant r<1)$; the interaction reduced energy

$$E_n^*=\sum_{i=1}^{z}\epsilon_{jk}^*(i)$$

is calculated over all z nearest neighbors. If $p>r$ the move is performed and the motion of a new monomer is attempted. This method of calculating the Boltzmann factor has been shown to yield results properly accounting for dynamic properties of dense polymer systems [8], and can be thought of as a dynamic Monte Carlo method.

Moreover, for 3-24-3 microarchitecture, we have also applied the standard Metropolis algorithm [30] when calculating the Boltzmann factor for cooperative chain moves. The numerical results for this microarchitecture were the same, within the statistical error, with both the dynamic Monte Carlo and the standard Metropolis Monte Carlo methods.

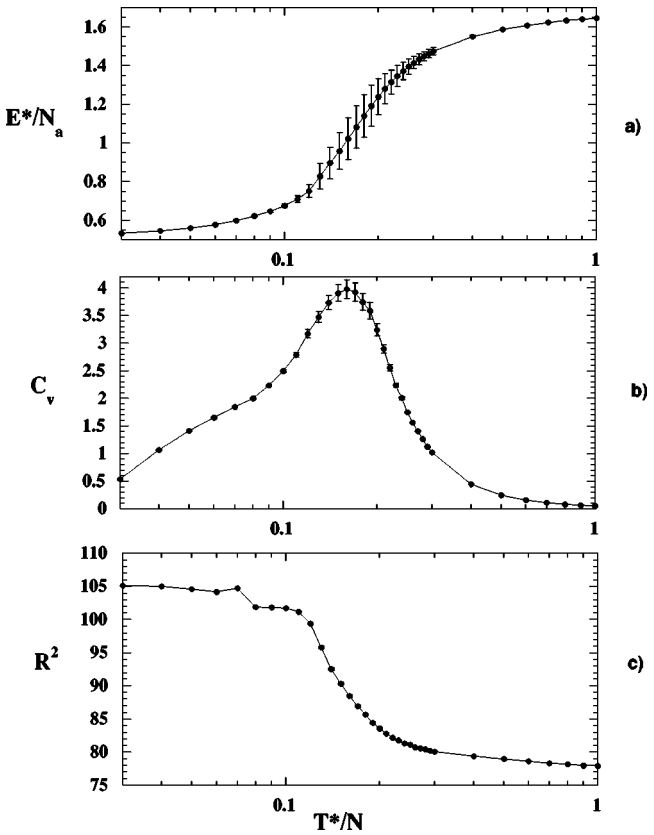

FIG. 3. Simulation results for the 3-24-3 microarchitecture (a) energy per lattice site, E^*/N_a, (b) specific heat C_v, (c) squared end-to-end distance R^2.

III. RESULTS

We start the simulation by equilibrating the system in the athermal limit, that is the state where $\epsilon/(k_BT)$ is zero. When the system reaches its thermal equilibrium the segments of different types are distributed uniformly within the simulation box. Then a jump is made to a finite reduced temperature $T^*/N=1$, at which the system still remains disordered. From this temperature the system is gradually cooled down, and we monitor the relevant properties which could indicate the ODT. For each temperature we perform 2×10^6 Monte Carlo time steps on the $60\times30\times30$ fcc lattice, and for each microarchitecture we perform three independent simulation experiments in order to improve the statistics, and verify reproducibility.

First, we present the results for the 3-24-3 triblock copolymer. In Fig. 3 we report the total energy per lattice site $e^*=E^*/N_a$, the specific heat, calculated as $C_v=\langle(e^*-\langle e^*\rangle)^2\rangle/T^*$, and the variations of the equilibrium end-to-end distance of triblock chain R^2 as a function of the reduced temperature. The reduced temperature T^* is divided by N, since according to Leibler's random-phase approximation theory [11] the ODT temperature T^*_{ODT} scales linearly with the number of segments, N. At high temperatures, we can confirm that, due to the excluded volume screening, the squared end-to-end distance of the copolymer chain is quite close to the ideal Gaussian value $(N-1)a^2=58$, and as we decrease the temperature towards the ODT it increases significantly indicating chain extension. By examining Fig. 3(c), one can conclude that T^*_{ODT}/N is about 0.16. Similarly, by looking at the maximum of the specific heat C_v from Fig. 3(b), one can confirm nearly the same ODT temperature.

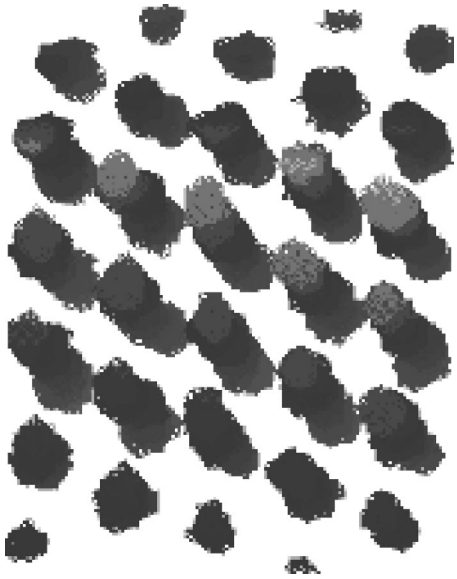

FIG. 4. A visualization of the 3-24-3 triblock copolymer at $T^*/N=0.03$, only A block monomers shown in four simulation boxes.

In Fig. 4 we present a visualization of an ordered microstructure for 3-24-3 microarchitecture at $T^*/N=0.03$. These are ordered cylinders shown in four simulation boxes, that is in the primary $60\times30\times30$ simulation box and its three neighboring periodic images. At higher temperatures, just below the ODT, we can see weakly segregated micelles. Recently Ryu and Lodge [17] have reported a reversible thermotropic cylinder-to-sphere transition for a poly(styrene-isoprene-styrene) triblock copolymer melt (15% styrene by volume). Spheres are observed at higher temperature and cylinders at lower temperature, which is what we report in this simulation for 3-24-3 triblock copolymer.

Similar simulations for 7-16-7 and 10-10-10 triblock copolymers have been performed. In Figs. 5, 6, and 7 we present some of the results for the 7-16-7 microarchitecture. As we can see from Fig. 5(c), at high temperatures the squared end-to-end distance is quite close to the ideal Gaussian value $(N-1)a^2=58$, and as we decrease the temperature towards the ODT it increases significantly. Similarly by looking at the maximum of the specific heat C_v, maximum from Fig. 5(b), one can confirm that T^*_{ODT}/N is about 0.28. The microarchitecture 7-16-7 is almost symmetrical with respect to A and B content, therefore we expect the lamellar morphology to be the equilibrium one. Indeed, from visualization of A monomers in 4 simulation boxes (the primary $60\times30\times30$ simulation box and its three neighboring periodic images) at $T^*/N=0.03$, in Fig. 6, we can notice very well developed layers at this low temperature. In Fig. 7(a) we show the distribution of the copolymer chain end-to-end distances in the direction normal to the layers at $T^*/N=0.03$. Shorter distances, i.e., smaller or equal to 5, correspond to the looped configuration, whereas the larger distances corre-

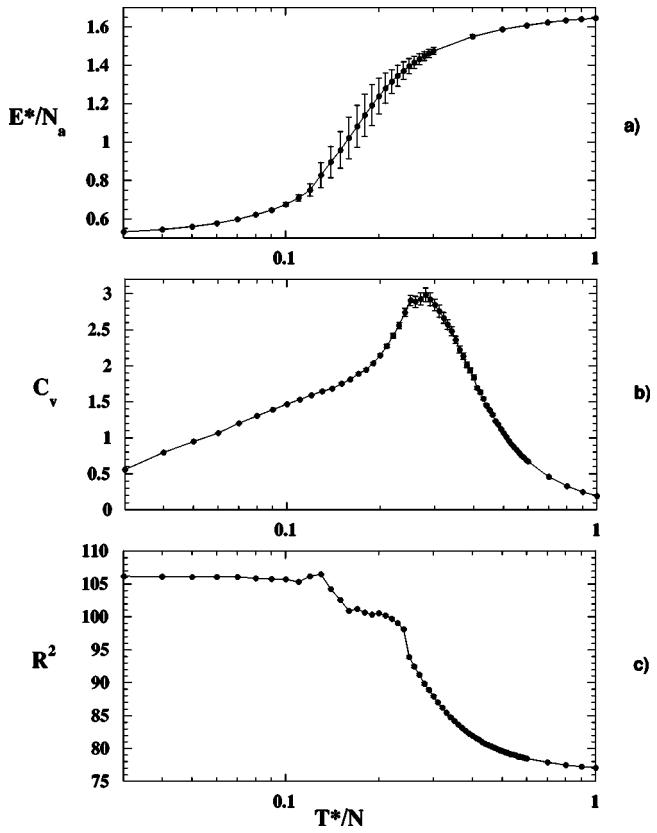

FIG. 5. Simulation results for the 7-16-7 microarchitecture: (a) energy per lattice site, E^*/N_a, (b) specific heat C_v, (c) squared end-to-end distance R^2.

spond to the bridged configurations. In Fig. 7(b) we report the bridging fraction as a function of the reduced temperature. Most experimental and theoretical studies point to a bridging fraction of about 40% [7,19,1,2], which is not far from what we have obtained at higher temperatures.

Finally, in Fig. 8 we present the results for the 10-10-10 microarchitecture. As before, we determine T^*_{ODT}/N to be

FIG. 6. A visualization of the 7-16-7 triblock copolymer at $T^*/N=0.03$, only A block monomers shown in four simulation boxes.

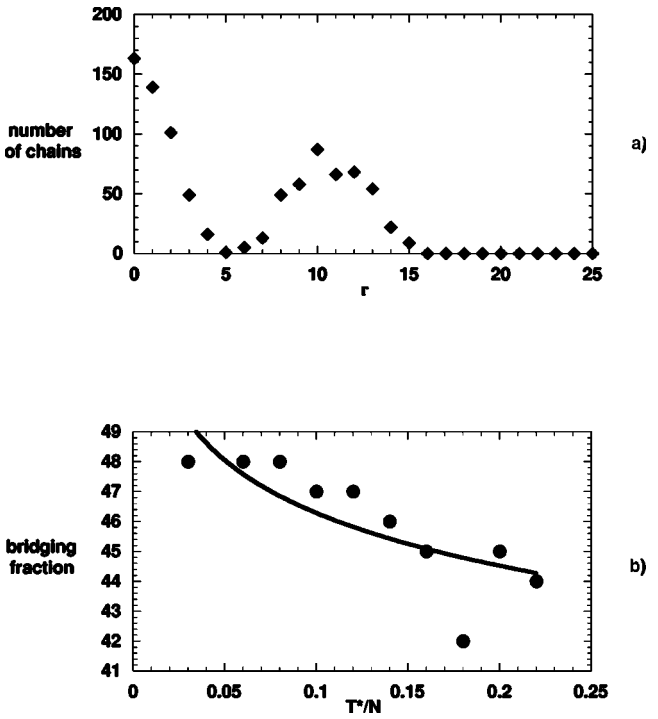

FIG. 7. Properties of the triblock chains in the lamellar microphase: (a) Distribution of end-to-end distance normal to layers at $T^*/N=0.03$. (b) Bridging fraction (in %) vs the reduced temperature T^*/N.

about 0.24 from the squared end-to-end copolymer chain distance, Fig. 8(c), and the specific heat, Fig. 8(b). Then, in Fig. 9 we present a visualization of the ordered microstructure at $T^*/N=0.03$, where we show only B block monomers (the minority middle block). This is a bicontinuous microstructure, where two distinct continuous components are shown in two different colors. In Fig. 9(a) we show just one continuous component, while in Fig. 9(b) we visualize both continuous components. We identify this microstructure as a bicontinuous double diamond structure. It is not completely unexpected to obtain the double diamond microstructure rather than a gyroid microstructure, because of the finite-size effects in our simulation, and small free energy differences between those two cubic bicontinuous microstructures, which have been reported in SCFT calculations.

In Fig. 10, we summarize our results by sketching a schematic phase diagram of the symmetric A-B-A triblock copolymers. If f denotes the fraction of A monomers, which are the external block monomers, then it is known from the SCFT calculations [5] and experimental data [18], that the phase diagram is roughly symmetric with respect to changing f to $(1-f)$. We show the ODT temperatures for three compositions: $f=6/30$, $f=14/30$, and $f=20/30$, corresponding to microarchitectures 3-24-3, 7-16-7, and 10-10-10, respectively. Furthermore we indicate microphases for those compositions at $T^*/N=0.03$ by labeling them C, L, and B, for cylindrical, lamellar and bicontinuous microphases, respectively. We also display, using the very rough symmetry, points C', L', and B', which are the mirror images of points C, L, and B with respect to $f=1/2$ composition, and similarly

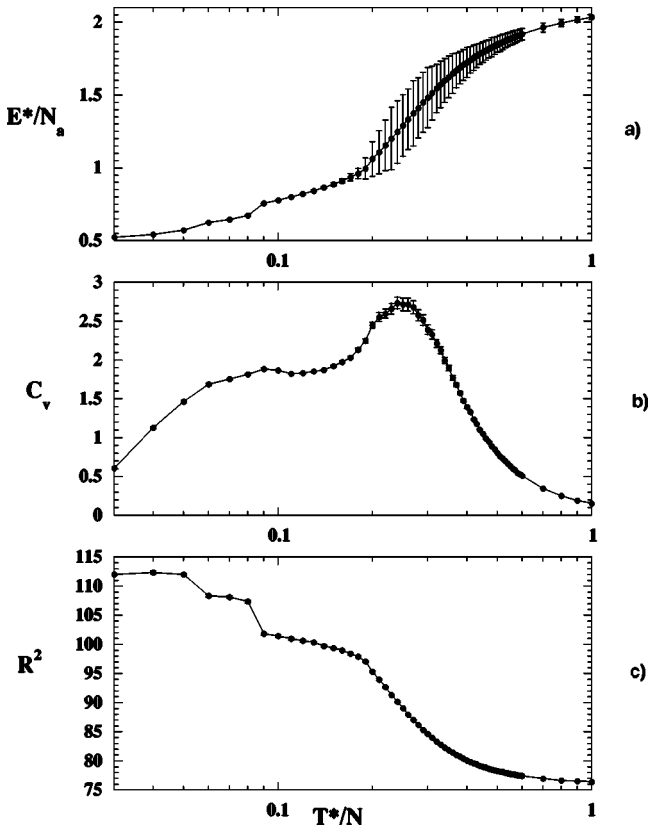

FIG. 8. Simulation results for the 10-10-10 microarchitecture: (a) energy per lattice site, E^*/N_a, (b) specific heat C_v, (c) squared end-to-end distance R^2.

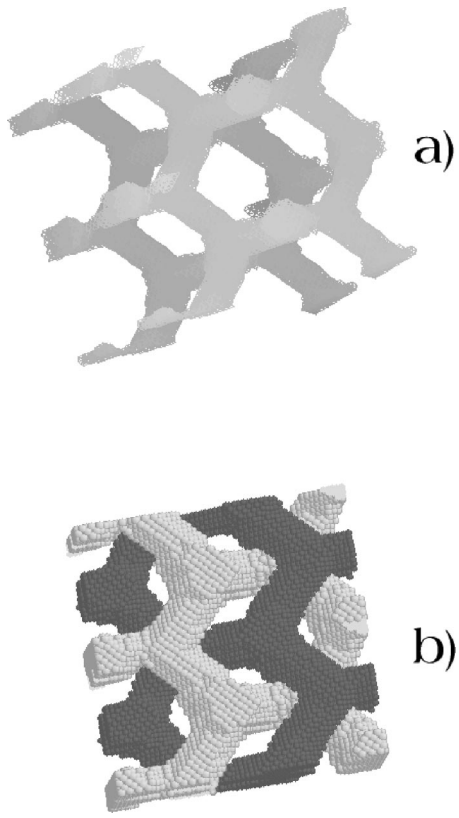

FIG. 9. A visualization of the 10-10-10 triblock copolymer at $T^*/N=0.03$, only *B* block monomers shown in four simulation boxes: (a) one continuous component, (b) two continuous components.

we display the ODT temperatures at compositions $f=24/30$, 16/30, and 10/30. It should be stressed that data at compositions $f=24/30$, 16/30, and 10/30 are not simulation results but only reasonable guesses based on theory and experiment [5,18]. All these data, both the simulation data at $f=6/30$, 14/30, and 20/30, and the corresponding guesses, give us an approximate outline of the phase diagram for the symmetric *A*-*B*-*A* triblock copolymer.

IV. CONCLUSION

We have demonstrated that varying systematically the microarchitecture and the temperature of a symmetric triblock copolymers of type *A*-*B*-*A* produces a series of interesting ordered microstructures, i.e., lamellar microstructure for 7-16-7 microarchitecture, double diamond microstructure for 10-10-10 microarchitecture, and cylindrical and weakly segregated spherical microstructures for 3-24-3 microarchitecture. We have been able to estimate order-disorder transition temperature T^*_{ODT}/N, from energy, specific heat, and end-to-end distance measurements. In order to determine the accurate phase boundaries further investigations are needed. In particular, precise methods of discriminating the microphases are required. Copolymer phase behavior is controlled by both enthalpic and entropic contributions, and in order to capture the entropic penalties of stretching different chains one needs to have blocks with a large number of segments. In the three ''samples'' considered, that is 3-24-3, 7-16-7, and 10-10-10, both the total copolymer chain length $N=30$ and the individual block lengths, e.g., $N_A=3$, are small. At this moment we are limited by available computing power, but with increasing resources, copolymer melts with significantly larger molecular weights can be simulated within larger boxes.

The cooperative motion algorithm, the simulation method used in this study, realistically represents a dense copolymer melt taking into account hard core interactions, polymer connectivity, and chain entanglements. Neverthe-

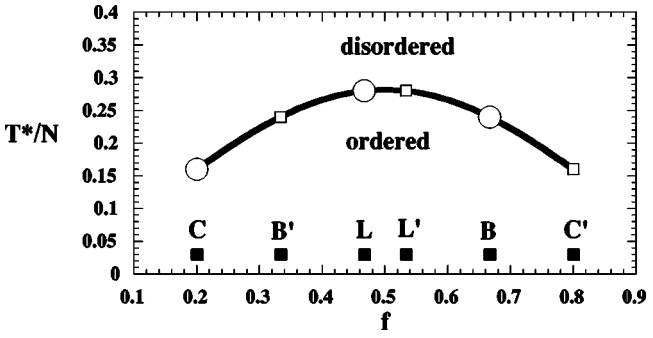

FIG. 10. Schematic phase diagram for symmetric *A*-*B*-*A* triblock copolymer: *C*, cylindrical microphase: *B*, bicontinuous microphase; and L, lamellar. Points C', B', and L' are symmetrical images of *C*, *B*, and *L*, respectively.

less, the results obtained are subject to the current limitations of the lattice Monte Carlo simulations of block copolymer self-assembly. The major difficulty in copolymer simulations is the competition of different length scales, i.e., simulation box size, microstructure periodicity, fluctuation correlation length. The choice of the simulation box lengths is, therefore, particularly important, as it should be significantly larger than the microstructure periodicity. In this work we have used a very slow cooling scheme with very long equilibration times to ensure that the true equilibrium structure and periodicity are achieved. In principle, there is a variety of microstructures which are commensurate with the simulation box size, and thus many possible periodicities. For lamellar microstructure, if the layers were to orient only along $(k00)$ plane of the simulation box, where k is an integer, then one would have to choose the box size very precisely, but since they can orient themselves along any commensurate plane, they have quite a lot of freedom in choosing their periodicity, provided the box length is at least about 5 to 10 times larger than the periodicity. If, for example, the layer thickness is 1/5 of the box length, then the layers can be oriented along (500) plane or (430) plane. If, however, the equilibrium layer thickness is slightly larger than 1/5 of the box length, then the layers can also be oriented along (422) plane, and then it is shifted by only about 2%. We have also noticed in our simulation experiments, that once the orientation is locked, it is very difficult to change it, probably due to high energy barriers, and as a result the lamellar periodicity does not vary much as we slowly cool down the triblock melt. This behavior is different from the expected lamellar periodicity expansion upon cooling, and consequently the bridging fraction does not decrease upon cooling as predicted by theory [33].

In our next study we perform the simulations in a different way. Instead of series of slow and long coolings, we perform a series of quenches where the triblock melt is cooled down instantaneously from $T^*/N=1.0$ to the required reduced temperature T^*/N. This alternative method gives results very similar to that of the slow cooling as far as the thermodynamic properties are concerned, but yields quite different structural data because the layer thickness is not locked to its high-temperature (near T_{ODT}) value. In particular, it shows that the layer thickness increases with decreasing temperature, as predicted by theoretical calculation, scaling nearly as $(T^*)^{-1/6}$, and the bridging fraction decreases, scaling nearly as $(T^*)^{1/9}$ in close agreement with theory [33]. These quenching simulation experiments are underway, and will be reported in a future publication. We also intend to present a simulation of complex microphases formation, such as the gyroid microphase, and to explore systematically the finite-size effects by probing different box sizes and shapes, and also copolymer molecular weights.

ACKNOWLEDGMENTS

M.B. acknowledges partial support by the Polish Committee for Scientific Research (KBN), Project No. 8T11F 01214.

[1] M.W. Matsen and M. Schick, Macromolecules **27**, 187 (1994).
[2] M.W. Matsen, J. Chem. Phys. **102**, 3884 (1995).
[3] W. Zheng and Z.-G. Wang, Macromolecules **28**, 7215 (1995).
[4] M.W. Matsen, J. Chem. Phys. **108**, 785 (1997).
[5] M.W. Matsen and R.B. Thomson, J. Chem. Phys. **111**, 7139 (1999).
[6] A.K. Khandpur, S. Forster, F.S. Bates, I.W. Hamley, A.J. Ryan, W. Bras, K. Almdal, and K. Mortensen, Macromolecules **28**, 8796 (1995).
[7] H. Watanabe, Macromolecules **28**, 5006 (1995).
[8] T. Pakula, J. Comput.-Aided Mater. Des. **3**, 351 (1996).
[9] T. Pakula, K. Karatasos, S.H. Anastasiadis, and G. Fytas, Macromolecules **26**, 8463 (1997).
[10] A. Weyersberg and T.A. Vilgis, Phys. Rev. E **48**, 377 (1993).
[11] L. Leibler, Macromolecules **13**, 1602 (1980).
[12] M.W. Matsen and F.S. Bates, Macromolecules **29**, 1091 (1996).
[13] M. Laradji, A.-C. Shi, J. Noolandi, and R.C. Desai, Macromolecules **30**, 3242 (1997).
[14] M. Banaszak and J.H.R. Clarke, Phys. Rev. E **60**, 5753 (1999).
[15] T. Dotera and H. Hatano, J. Chem. Phys. **105**, 8413 (1996).
[16] T. Dotera, Phys. Rev. Lett. **82**, 105 (1999).
[17] C.Y. Ryu and T.P. Lodge, Macromolecules **32**, 7190 (1999).
[18] S.-M. Mai, W. Mingvanish, S.C. Turner, C. Chaibundit, J.P.A. Fairclough, F. Heatley, M.W. Matsen, A.J. Ryan, and C. Booth, Macromolecules **33**, 5124 (2000).
[19] K. Karatassos, S.H. Anastasiadis, T. Pakula, and H. Watanabe, Macromolecules **33**, 523 (2000).
[20] A.V. Dobrynin and I.Y. Erukhimovich, Macromolecules **26**, 276 (1993).
[21] A.M. Mayes and M.O. de la Cruz, J. Chem. Phys. **95**, 4670 (1991).
[22] U. Micka and K. Binder, Macromol. Theory Simul. **4**, 419 (1995).
[23] H. Fried and K. Binder, J. Chem. Phys. **94**, 8349 (1991).
[24] S. Phan and G.H. Fredrickson, Macromolecules **31**, 59 (1998).
[25] R. Larson, Macromolecules **27**, 4198 (1994).
[26] J. Huh, W.H. Jo, and G. ten Brinke, Macromolecules **35**, 2413 (2002).
[27] F. Drolet and G.H. Fredrickson, Macromolecules **34**, 5317 (2001).
[28] R.D. Groot and T.J. Madden, J. Chem. Phys. **108**, 8713 (1998).
[29] G.H. Fredrickson, V. Ganesan, and F. Drolet, Macromolecules **35**, 2002 (2002).
[30] N. Metropolis, A.W. Rosenbluth, M.N. Rosenbluth, A.H. Teller, and E. Teller, J. Chem. Phys. **21**, 1087 (1953).
[31] G.S. Grest, M.-D. Lacasse, K. Binder, and A.M. Gupta, J. Chem. Phys. **105**, 10 583 (1996).
[32] M. Banaszak and J.H.R. Clarke (unpublished).
[33] A. Halperin and E.B. Zhulina, Europhys. Lett. **16**, 337 (1991).